[CANCER RESEARCH 64, 7668–7672, November 1, 2004]

Advances in Brief

Nanoparticle-Aptamer Bioconjugates: A New Approach for Targeting Prostate Cancer Cells

Omid C. Farokhzad,[1,2] Sangyong Jon,[3] Ali Khademhosseini,[4] Thanh-Nga T. Tran,[2] David A. LaVan,[2] and Robert Langer[2,4,5,6]

[1]Department of Anesthesiology, Brigham and Women's Hospital, Boston, Massachusetts; [2]Division of Health Sciences and Technology, Massachusetts Institute of Technology, Cambridge, Massachusetts; [3]Department of Life Science, Gwangju Institute of Science & Technology, Gwangju, South Korea; and [4]Division of Biological Engineering, [5]Department of Chemical Engineering, and [6]Center for Cancer Research, Massachusetts Institute of Technology, Cambridge, Massachusetts

Abstract

Nucleic acid ligands (aptamers) are potentially well suited for the therapeutic targeting of drug encapsulated controlled release polymer particles in a cell- or tissue-specific manner. We synthesized a bioconjugate composed of controlled release polymer nanoparticles and aptamers and examined its efficacy for targeted delivery to prostate cancer cells. Specifically, we synthesized poly(lactic acid)-block-polyethylene glycol (PEG) copolymer with a terminal carboxylic acid functional group (PLA-PEG-COOH), and encapsulated rhodamine-labeled dextran (as a model drug) within PLA-PEG-COOH nanoparticles. These nanoparticles have the following desirable characteristics: (*a*) negative surface charge (-50 ± 3 mV, mean ± SD, $n = 3$), which may minimize nonspecific interaction with the negatively charged nucleic acid aptamers; (*b*) carboxylic acid groups on the particle surface for potential modification and covalent conjugation to amine-modified aptamers; and (*c*) presence of PEG on particle surface, which enhances circulating half-life while contributing to decreased uptake in nontargeted cells. Next, we generated nanoparticle-aptamer bioconjugates with RNA aptamers that bind to the prostate-specific membrane antigen, a well-known prostate cancer tumor marker that is overexpressed on prostate acinar epithelial cells. We demonstrated that these bioconjugates can efficiently target and get taken up by the prostate LNCaP epithelial cells, which express the prostate-specific membrane antigen protein (77-fold increase in binding *versus* control, $n = 150$ cells per group). In contrast to LNCaP cells, the uptake of these particles is not enhanced in cells that do not express the prostate-specific membrane antigen protein. To our knowledge, this represents the first report of targeted drug delivery with nanoparticle-aptamer bioconjugates.

Introduction

The combination of targeted delivery and controlled drug release (1, 2) are potentially desirable properties when treating oncologic diseases where it is desirable that a cytotoxic dose of the drug is delivered to cancer cells over an extended period of time without killing the surrounding noncancerous tissue. Critical to achieving this goal is the engineering of specialized vehicles that encapsulate chemotherapeutic drugs for controlled release, and the targeting of these vehicles to cancer cells with ligands that recognize tumor-specific or tumor-associated antigens. A wide variety of targeting molecules have been assessed, with varying degrees of success, for their potential application in cancer therapy, including humanized antibodies and single-chain Fv generated from murine hybridoma or phage display, minibodies, and peptides (3). Interestingly, nucleic acid ligands, also called aptamers (4, 5), have emerged as a novel class of ligands that rival antibodies in their potential for therapeutic and diagnostic applications (6, 7). Aptamers are RNA or DNA oligonucleotides that fold by intramolecular interaction into unique three-dimensional conformations capable of binding to target antigens with high affinity and specificity. Considering the many favorable characteristics of aptamers, including small size, lack of immunogenicity, and ease of isolation, which together has resulted in their rapid progress into clinical trials (8), we became interested in examining these molecules for targeted delivery of controlled release polymer drug delivery vehicles.

As proof of concept we used RNA aptamers that bind to the prostate-specific membrane antigen (PSMA; ref. 9), a well-known transmembrane protein that is overexpressed on prostate cancer epithelial cells (10, 11), to develop specialized nanoparticle-aptamer bioconjugates for targeted delivery to prostate cancer cells. Prostate cancer is the single most common form of non–skin malignancy in men in the United States (12), and vehicles that target this disease for therapy may have a role in the management of this disease (13, 14). We used the following criteria for the development of our delivery vehicles: first, we were interested in developing drug encapsulated particles with a polymer system with components that were biocompatible, biodegradable, and approved by the Food and Drug Administration for a prior clinical use. Second, we were interested in developing particles that could be efficiently linked to the negatively charged nucleic acid aptamers using simple chemistry with minimal to no adverse effect on the three-dimensional conformation and ligand recognition properties of aptamers. Third, we were interested in developing delivery vehicles that demonstrate differentially high uptake efficiency by the targeted cells. Fourth, we were interested in developing vehicles with extended circulating half-life to increase the likelihood of their effectiveness in future therapeutic applications (15). We used rhodamine-labeled dextran (as a model drug) and developed drug encapsulated pegylated PLA nanoparticles with a negative surface charge. Using the PSMA aptamer, we developed nanoparticle-aptamer bioconjugates and then examined whether the targeting and uptake of these vehicles by prostate epithelial cells, which express the PSMA protein, could be achieved.

Materials and Methods

Materials. All chemicals were obtained from Sigma-Aldrich (St. Louis, MO) unless otherwise noted. Poly($_{D,L}$-lactic acid) (PLA; average M_r 25,000) was purchased from Boehringer Ingelheim (Ingelheim, Germany). The polyethylene glycol (PEG) polymer with a terminal hydroxyl and carboxylic acid functional groups (OH-PEG$_{3400}$-COOH) was custom synthesized by Nektar Therapeutics (San Carlos, CA).

Synthesis of PLA-PEG-COOH. The $_{D,L}$-lactide and OH-PEG$_{3400}$-COOH were used to synthesize poly($_{D,L}$-lactic acid)-*block*-polyethylene glycol-COOH copolymer (PLAPEG-COOH) by ring opening polymerization. The PLA-PEG$_{3400}$-COOH was characterized by ^{1}H-NMR (400 MHz), $\delta = 5.28–5.11$

Received 7/16/04; accepted 9/15/04.

Grant support: The David H. Koch Research Fund and the Foundation for Anesthesia Education and Research.

The costs of publication of this article were defrayed in part by the payment of page charges. This article must therefore be hereby marked *advertisement* in accordance with 18 U.S.C. Section 1734 solely to indicate this fact.

Requests for reprints: Robert Langer, Kenneth J. Germeshausen Professor of Chemical and Biomedical Engineering, Massachusetts Institute of Technology, Building E25–342, 45 Carleton Street, Cambridge, MA 02139. Phone: (617) 253-3123; Fax: (617) 258-8827; E-mail: rlanger@mit.edu.

(br, -OC-C*H*(CH_3)O- in PLA), 3.62 (s, -CH_2CH_2O- in PEG), 1.57–1.45 (br, -OC-CHCH_3O- in PLA); molecular weight (GPC): M_n = 10,500 with M_w/M_n = 1.54 relative to monodispersed polystyrene standards.

Nanoparticles. Drug encapsulated nanoparticles were prepared using the water-in-oil-in-water solvent evaporation procedure (double emulsion method) as described previously (15). The size (nm) and surface charge (ζ potential in mV) of nanoparticles were evaluated by Quasi-elastic laser light scattering with a ZetaPALS dynamic light scattering detector (Brookhaven Instruments Corporation, Holtsville, NY; 15 mW laser, incident beam = 676 nm). Surface morphology and size were also determined by high-resolution scanning electron microscopy (JEOL 6320FV).

Nanoparticle-Aptamer Conjugation. Fifty microliters of PLA-PEG-COOH nanoparticle or microparticle suspension (~10 μg/μL in DNase RNase-free water) was incubated with 200 μL of 400 mmol/L 1-(3-dimethylaminopropyl)-3-ethylcarbodimide hydrochloride (EDC) and 200 μL of 100 mmol/L *N*-hydroxysuccinimide (NHS) for 15 minutes at room temperature with gentle stirring. The resulting NHS-activated particles were covalently linked to 50 μL of 3′-NH_2–modified A10 PSMA aptamer (ref. 9; 1 μg/μL in DNase RNase-free water) or 3′-NH_2 and 5′-FITC–modified A10 PSMA aptamer where indicated. The resulting aptamer-nanoparticle bioconjugates were washed, resuspended, and preserved in suspension form in DNase RNase-free water. The conjugation of 5′-FITC and 3′-NH_2–modified A10 PSMA aptamer to PLA-PEG-COOH nanoparticles and microparticles (0.5 mg/mL) was analyzed with the FACScan flow cytometer (Becton Dickinson, San Jose, CA) and fluorescent microscopy, respectively.

Cellular Binding and Uptake Studies. The prostate LNCaP and PC3 cell lines were grown in chamber slides in RPMI 1640 and Ham's F12K medium, respectively, supplemented with 100 units/mL aqueous penicillin G, 100 μg/mL streptomycin, and 10% fetal bovine serum at concentrations to allow 70% confluence in 24 h (*i.e.,* LNCaP: 40,000 cells/cm^2). On the day of experiments, cells were washed with prewarmed PBS and incubated with prewarmed phenol-red–reduced OptiMEM media for 30 minutes before the addition of 50 μg of nanoparticle-aptamer bioconjugates. Cells were incubated for 75 minutes to 16 hours at 37°C, washed with PBS three times, fixed with 4% paraformaldehyde, counterstained with 4′,6-diamidino-2-phenylindole and Alexa-Flour Phalloidin, mounted, and visualized by fluorescent microscopy. Where indicated, the number of nanoparticle aptamer bioconjugates or control nanoparticles attached to individual LNCaP or PC3 cells was quantified by fluorescent microscopy under oil immersion at 100× magnification. For pseudoconfocal imaging, cells were visualized with a 1.4 numerical aperature oil immersion 100× objective, and individual images were taken along their z-axis at 0.1-μm intervals with a computerized Zeiss Axiovert 200M microscope (Carl Zeiss Microimaging, Thornwood, NY). Images were combined and deconvoluted to reconstruct a three-dimensional image of the cells for additional analysis

Prostate Cancer Tissue Staining. After antigen retrieval, formalin-fixed, paraffin-embedded prostate cancer tissue slides (Clinomics Biosciences, Watervliet, NY) were incubated with biotin-labeled A10 PSMA aptamer in 1 mL of PBS in the presence of 5× molar excess of tRNA and 0.2% BSA for 30 minutes at 37°C. Slides were washed with PBS three times and incubated with horseradish peroxidase-conjugated streptavidin for 1 hour, washed with PBS three times, incubated with the peroxidase substrate, washed with PBS twice, mounted, and analyzed by light microscopy.

Results and Discussion

Development of Controlled Release Polymer Drug Delivery Vehicles Suitable for Conjugation to Aptamers. We chose to generate particles with PLA and its derivatives. Particles that are generated from PLA are expected to have a neutral to slightly negative surface charge, a desirable characteristic because particles with a positive surface charge may nonspecifically interact with the negatively charged aptamers and diminish their binding characteristics. We hypothesized that by modifying the terminal ends of polymers with a hydrophilic carboxylic acid functional group, we may provide additional negative charge on particles that could repel the similarly charged aptamers and minimize charge interaction between the aptamers and particle surface. In addition, the presence of the carboxylic acid group on the particle surface would allow an easy conversion to NHS ester for covalent linkage to NH_2-modified aptamers. We also decided to incorporate PEG in generating pegylated nanoparticle-aptamer bioconjugates. PEG has been shown to prolong nanoparticle circulating half-life (15), presumably because of the ability of PEG to reduce nonspecific adsorption of biomacromolecules such as proteins and nucleic acid (16). This latter characteristic may also contribute to minimizing nonspecific interaction of conjugated aptamers with the nanoparticle surface.

We used the following two polymer systems to generate nanoparticles and microparticles: PLA and pegylated PLA with a terminal carboxylic acid functional group (PLA-PEG-COOH). Particles were characterized for their size, surface charge (ζ potential), and surface morphology with Quasi-elastic laser light scattering, ZetaPALS dynamic light scattering detector, and scanning electron microscopy, respectively. The nanoparticles generated from both polymer systems showed narrow size distribution (polydispersity index < 0.1). The ζ potential of the PLA-PEG-COOH nanoparticles and microparticles were significantly more negative than the unmodified PLA particles as predicted (−50 ± 3 mV, mean ± SD, n = 3). The surface morphology and size distribution of particles from both polymer systems were determined by scanning electron microscopy, and representative images of PLA-PEG-COOH nanoparticles and microparticles were shown (Fig. 1).

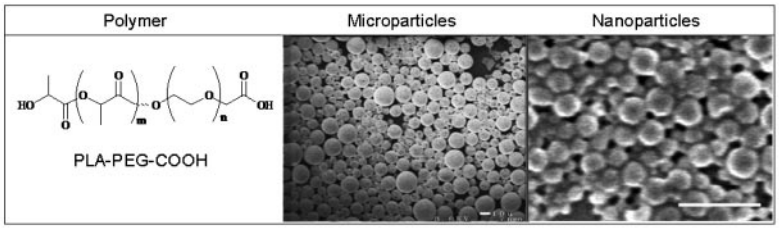

Fig. 1. PLA-PEG-COOH polymer was dissolved in dichloromethane, and an aqueous solution of rhodamine-labeled dextran (as a model drug) was added, and the mixture emulsified with a probe sonicator. Polyvinyl alcohol solution was added and a second emulsion was prepared by sonication to make nanoparticles or by mechanical stirring to make microparticles. Organic solvent was evaporated from emulsion and the nano- or microparticles were washed with deionized water and collected by centrifugation. The surface morphology and size distribution of microparticles (*left panel*) and nanoparticles (*right panel*) was examined by scanning electron microscopy (*white bar* represents 1 μm). The chemical structure of the PLA-PEG-COOH polymer system is represented on the left. The data representing mean particle size and ζ potential of particles from each polymer system was summarized (mean ± SD; n = 3; *P > 0.001).

Polymer System	Mean Size (nm)[§]	Zeta Potential (mV)[§]
PLA	252 ± 11 [†]	-24 ± 5
PLA	2420 ± 270 [††]	-23 ± 9
PLA-PEG-COOH	249 ± 12 [†]	-50 ± 3 *
PLA-PEG-COOH	2805 ± 301 [††]	-51 ± 2 *

*[§]Data represents mean ± SD, N = 3. [†]Nanoparticles and [††]microparticles. *Significantly different from PLA (P>0.001).*

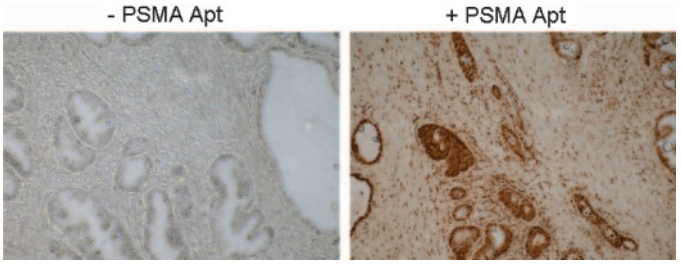

Fig. 2. Formalin-fixed, paraffin-embedded prostate cancer slides were stained in the absence (−PSMA Apt) or presence (+PSMA Apt) of biotinylated A10 PSMA aptamer for 30 minutes. Slides were washed with PBS twice, incubated with streptavidin-horseradish peroxidase for 10 minutes, washed with PBS twice, incubated with the peroxidase substrate, washed with PBS twice, mounted, and analyzed by light microscopy. Cells which express the PSMA protein are stained in brown.

Development of Nanoparticle-Aptamer Bioconjugate for Targeted Drug Delivery to Prostate Cancer Cells. Two RNA aptamers were previously selected against the extracellular region of the PSMA protein (9). One aptamer, A10, has 2′-fluoro–modified ribose on all pyrimidines and a 3′-inverted deoxythymidine cap, which together confer significant nuclease resistance to this molecule. Because we are interested in developing a methodology for using aptamers to target the delivery of controlled released polymer particles to specific cells together with the fact that PSMA represents a well-characterized target of significant importance in prostate cancer, we used the A10 PSMA aptamer to generate our nanoparticle-aptamer bioconjugates. We demonstrated that consistent with the original report (9), the binding activity of A10 PSMA aptamer is restricted to LNCaP cells, which express the PSMA but not PC3 cells, which do not express the PSMA protein (data not shown). We then demonstrated that the A10 aptamer binds to the acinar epithelial cells of prostate cancer tissue consistent with the expected pattern of PSMA expression in the prostate gland (Fig. 2).

Using the PLA-PEG-COOH nano- and microparticles and the A10 PSMA aptamer, we generated nanoparticle-aptamer and microparticle-aptamer bioconjugates for the assessment of our conjugation strategy (Fig. 3*A*). To examine the presence of the aptamers on particle surface, we used A10 PSMA aptamer with a 5′-FITC-label and a 3′-NH_2 modification to yield fluorescent nanoparticle-aptamer and microparticle-aptamer bioconjugates. The acid group on the particle surface was first converted to NHS ester in the presence of EDC and subsequently was covalently coupled to the amine-modified aptamer. To assess the specificity of aptamer interaction with the particle surface, we incubated aptamers with nanoparticles and microparticles without the conversion of carboxylic acid to NHS ester (*i.e.,* absence of EDC); thus, any interaction would be nonspecific (*i.e.,* charge or hydrogen bond interaction). The microparticle-aptamer bioconjugates were characterized by microscopy (Fig. 3*B*) and given the size limitations, the nanoparticle-aptamer bioconjugates were characterized by flow cytometry (Fig. 3*C*). These data demonstrate the specificity of our conjugation reaction.

Nanoparticle-Aptamer Bioconjugates Selectively and Efficiently Deliver Drugs to Targeted Cells. Through time course studies, we next demonstrated that the binding of pegylated nanoparticle-aptamer bioconjugates to LNCaP cells was significantly enhanced when compared with control pegylated nanoparticles lacking the A10 PSMA aptamer (Fig. 4*A*, top). In the case of PC3 prostate epithelial cells, which do not express the PSMA protein, no measurable difference in binding was observed between the bioconjugate and the control group (Fig. 4*A*, bottom). The number of nanoparticles attaching to representative cells after 75 minutes incubation of bioconjugates or control nanoparticles with LNCaP or PC3 cells was quantified by fluorescent microscopy. The data demonstrates a 77-fold enhancement in the binding of bioconjugates *versus* the control group in LNCaP cells (13.25 ± 7.56 *versus* 0.17 ± 0.45 nanoparticles per cell for bioconjugates *versus* control group, respectively; mean ± SD, $n = 150$, $P > 0.001$). A notable observation was a remarkably low binding efficiency of nanoparticles in nontargeted PC3 cells (0.03 ± 0.18 *versus* 0.30 ± 0.62 nanoparticles per cell for bioconjugates *versus* control group; mean ± SD, $n = 150$), presumably attributed to the presence of the PEG group (16, 17). The binding of bioconjugates to LNCaP cells was clearly detectable at the early time points; however, by 16 hours, the differential binding of nanoparticle-aptamer bioconjugates *versus* control group became markedly pronounced.

An antibody-mediated enhancement in the rate of PSMA endocytosis in LNCaP cells had previously been reported (18), and we were able to detect a measurable but a relatively modest enhancement in the

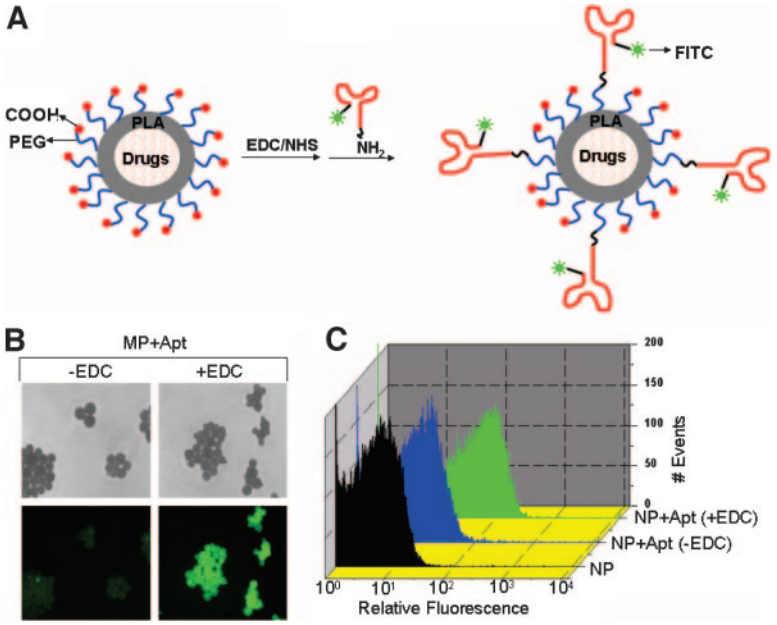

Fig. 3. *A*, schematic diagram of the conjugation reaction of PLA-PEG-COOH nanoparticles or microparticles with 3′-NH_2–modified, 5′-FITC–labeled PSMA aptamers. *B*, conjugation of microparticles with aptamers. The acid group on the surface of PLA-PEG-COOH microparticles (MP) were left untreated (−EDC) or converted to NHS ester (+EDC) and particles were incubated with NH_2-modified FITC-labeled PSMA aptamers. After the wash, the microparticles resulting after nonspecific interaction with aptamers (−EDC) or after covalent linkage with aptamers (+EDC) were visualized by transmission light microscopy (*top row*) and fluorescent microscopy (*bottom row*). *C*, conjugation of nanoparticles with aptamers. The acid group on the surface of PLA-PEG-COOH nanoparticles were left untreated (−EDC) or converted to NHS ester (+EDC), and particles were examined without aptamers (NP, *black curve*) or incubated with NH_2-modified FITC-labeled aptamers (+Apt). The bioconjugates resulting from the covalent linkage of aptamers and nanoparticles [NP+Apt (+EDC, *green curve*)] demonstrated an approximate 7-fold increase in fluorescence when compared with nanoparticles that were incubated but had no covalent linkage to aptamers [NP+Apt (−EDC, *blue curve*)].

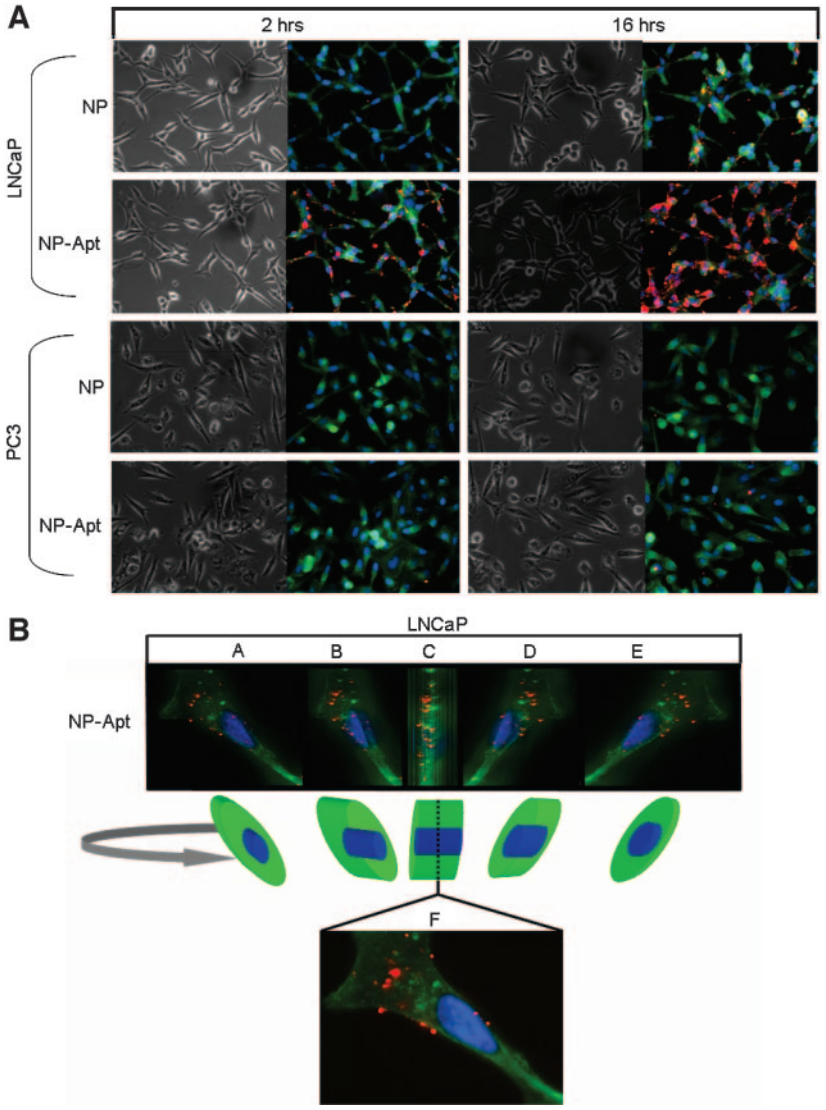

Fig. 4. *A*, binding of nanoparticle-aptamer bioconjugates to prostate epithelial cells. LNCaP cells and PC3 cells were grown on chamber slides and incubated in culture medium supplemented with 50 μg of rhodamine-labeled dextran encapsulated pegylated nanoparticles, or 50 μg of rhodamine-labeled dextran encapsulated pegylated nanoparticle-aptamer bioconjugates (NP-Apt) for 2 hours (*left panel*) or 16 hours (*right panel*). Cells were washed in PBS three times, fixed, and permeabilized, stained with 4′,6′-diamidino-2-phenylindole (nuclei) and Alexa-Flour Phalloidin (cytoskeleton), washed, and analyzed by light transmission or fluorescent microscopy. The rhodamine-dextran encapsulated nanoparticles or nanoparticle-aptamer bioconjugates are shown in red. *B*, evaluation of nanoparticle-aptamer bioconjugates uptake by LNCaP cells. LNCaP cells were grown on chamber slides and incubated in culture medium supplemented with rhodamine-dextran encapsulated nanoparticle-aptamer bioconjugates (50 μg) for 2 hours, washed, and analyzed at 100× magnification along their z-axis at 0.1 μm intervals by fluorescent microscopy. Approximately 150 individual images were combined to reconstruct a three-dimensional image of the cell. *A* through *E* represent the same LNCaP cell being rotated at 45-degree intervals. This rotation is schematically represented below each panel to show the position of cell and the axis of rotation. *F* represents a single image through mid z-axis point of cell demonstrating particles in mid cross-section of cell and confirming the intracellular position of particles. The cell nuclei and the actin cytoskeleton are stained with *blue* (4′,6-diamidino-2-phenylindole) and *green* (Alexa-Flour Phalloidin), respectively. The intracellular rhodamine-dextran encapsulated nanoparticle-aptamer bioconjugates are shown in *red*.

rate of PSMA endocytosis in response to the A10 PSMA aptamer binding to LNCaP cells.[7] We next examined if the binding of bioconjugates to LNCaP cells results in particle uptake. Using z-axis fluorescent microscopy and three-dimensional image reconstruction, we studied the localization of the nanoparticle-aptamer bioconjugates after incubation with LNCaP cells. The data demonstrate that even at 2 hours, the particles were largely internalized into cells (Fig. 4*B*). This differential uptake of bioconjugates by LNCaP *versus* PC3 cells was reproducibly observed with different passages of cells and nanoparticle-aptamer bioconjugate preparations.

In summary, aptamers are quickly emerging as a powerful class of ligands with utility in therapeutic applications. Specialized delivery vehicles that use these molecules for targeted delivery will likely have a role in future therapeutic modalities (19, 20). In this article, we have developed controlled release polymer drug delivery vehicles suitable for conjugation to aptamers and developed, as proof of concept, nanoparticle-aptamer bioconjugates, which target and are taken up by prostate cancer epithelial cells. These vehicles are potentially suitable for efficient and specific targeted delivery of chemotherapeutic drugs to prostate cancer cells, and additional *in vivo* studies are needed to determine the biodistribution of these vehicles after systemic administration. Once these vehicles are optimized, we postulate that a similar strategy may be used to develop nanoparticle aptamer bioconjugates for targeted drug delivery to a myriad of important human diseases.

[7] O.C. Farokhzad, S. Jon, and R. Langer, unpublished observation.

Acknowledgments

We thank Shulamit Levenberg, Daniel Anderson, Daniel Kohane, and Yadong Wang for helpful discussions.

References

1. Langer R. Drug delivery and targeting. Nature (Lond.) 1998;392:5–10.
2. Langer R. Drug delivery. Drugs on target. Science (Wash. DC) 2001;293:58–9.
3. Weiner LM, Adams GP. New approaches to antibody therapy. Oncogene 2000;19:6144–51.
4. Ellington AD, Szostak JW. In vitro selection of RNA molecules that bind specific ligands. Nature (Lond.) 1990;346:818–22.
5. Tuerk C, Gold L. Systematic evolution of ligands by exponential enrichment: RNA ligands to bacteriophage T4 DNA polymerase. Science (Wash. DC) 1990;249:505–10.
6. Ishida S, Usui T, Yamashiro K, et al. VEGF164-mediated inflammation is required for pathological, but not physiological, ischemia-induced retinal neovascularization. J Exp Med 2003;198:483–9.
7. Brody EN, Gold L. Aptamers as therapeutic and diagnostic agents. J Biotechnol 2000;74:5–13.
8. Vinores SA. Technology evaluation: pegaptanib, Eyetech/Pfizer. Curr Opin Mol Ther 2003;5:673–9.

9. Lupold SE, Hicke BJ, Lin Y, Coffey DS. Identification and characterization of nuclease-stabilized RNA molecules that bind human prostate cancer cells via the PSMA. Cancer Res 2002;62:4029–33.
10. Murphy GP, Elgamal AA, Su SL, Bostwick DG, Holmes EH. Current evaluation of the tissue localization and diagnostic utility of prostate specific membrane antigen. Cancer (Phila.) 1998;83:2259–69.
11. Israeli RS, Powell CT, Corr JG, Fair WR, Heston WD. Expression of the prostate-specific membrane antigen. Cancer Res 1994;54:1807–11.
12. Jemal A, Tiwari RC, Murray T, et al. Cancer statistics, 2004. CA - Cancer J Clin 2004;54:8–29.
13. Leach F. Targeting prostate-specific membrane antigen in cancer therapy: can molecular medicine be brought to the surface? Cancer Biol Ther 2004;3:
14. Bander NH, Nanus DM, Milowsky MI, Kostakoglu L, Vallabahajosula S, Goldsmith SJ. Targeted systemic therapy of prostate cancer with a monoclonal antibody to prostate-specific membrane antigen. Semin Oncol 2003;30:667–76.
15. Gref R, Minamitake Y, Peracchia MT, Trubetskoy V, Torchilin V, Langer R. Biodegradable long-circulating polymeric nanospheres. Science (Wash. DC) 1994; 263:1600–3.
16. Fenske DB, MacLachlan I, Cullis PR. Stabilized plasmid-lipid particles: a systemic gene therapy vector. Methods Enzymol 2002;346:36–71.
17. Iinuma H, Maruyama K, Okinaga K, et al. Intracellular targeting therapy of cisplatin-encapsulated transferrin-polyethylene glycol liposome on peritoneal dissemination of gastric cancer. Int J Cancer 2002;99:130–7.
18. Liu H, Rajasekaran AK, Moy P, et al. Constitutive and antibody-induced internalization of prostate- specific membrane antigen. Cancer Res 1998;58: 4055–60.
19. Willis MC, Collins BD, Zhang T, et al. Liposome-anchored vascular endothelial growth factor aptamers. Bioconjug Chem 1998;9:573–82.
20. Hicke BJ, Stephens AW. Escort aptamers: a delivery service for diagnosis and therapy. J Clin Investig 2000;106:923–8.